Ab Initio Molecular Dynamics Studies of Off-Center Displacements in CuCl

S. R. Bickham,[1] J. D. Kress,[1] L. A. Collins,[1] and R. Stumpf[2]
[1]*Theoretical Division, Los Alamos National Laboratory, Los Alamos, New Mexico 87545*
[2]*Computational Materials Group, Motorola, Los Alamos, New Mexico 87545*
(Received 16 December 1998)

The unusual properties of CuCl have previously been interpreted using models that focus either on anharmonicity or off-center displacements from the zinc blende structure. We use *ab initio* molecular dynamics to show that both are important in determining the behavior of CuCl. At low temperatures, most of the Cu ions are located in off-center sites along the (111) directions. The lattice undergoes a gradual transition from static to dynamic disorder with rising temperature. Increasing pressure favors the zinc blende structure, in agreement with recent Raman experiments.

PACS numbers: 61.50.Ah, 61.66.–f, 61.72.Ji, 71.15.Pd

CuCl is one of the most puzzling semiconductors due to its anomalous optical, thermal, and structural properties. At room temperature, the average structure corresponds to a zinc blende lattice, but its ionicity is just below the threshold where the face-centered or body-centered cubic structure is preferred [1]. The nearest-neighbor separation is also significantly smaller than the sum of the ionic radii [2], so there is a large overlap in the wave functions of the valence electrons. This produces a pseudo-Jahn-Teller s-d coupling between the conduction and valence bands that leads to off-center structural instabilities similar to those associated with vacancies, deep defects, and transition metal impurities in other semiconductors [3].

The zinc blende structure has two atoms per unit cell and is expected to exhibit one longitudinal-optic (LO) and one transverse-optic (TO) mode at $k \approx 0$ [4]. While one LO mode is indeed observed, Raman scattering, infrared absorption, and inelastic neutron scattering experiments find two modes with TO symmetry [2,5–8]. Like many zinc blende semiconductors, CuCl undergoes a negative thermal expansion at low temperatures [2], but this effect is much more pronounced than in other crystals. Neutron diffraction data also indicate that the Cu vibrations are very anharmonic, even at low temperatures [9,10]. Although the diffuse elastic scattering suggests a significant amount of disorder, it has not been established whether the disorder is static or dynamic. In either case, a statistical distribution of displaced Cu ions could not give rise to the observed diffuse background unless there is some degree of correlation [10]. Another indication of the importance of anharmonicity and disorder is the observation that CuCl undergoes a transition to a superionic conductor at temperatures above 720 K, with the Cu^+ ions becoming mobile within the anion sublattice [11,12].

Several models [4,5,7–10,12–14] have been introduced to explain the anomalous behavior of CuCl, with two receiving the most attention. The Fermi resonance model predicts that the TO(β) mode is formed through a third-order anharmonic interaction that repels an optical phonon out of a two-phonon combination band [8,14]. While this model is able to reproduce the frequencies, linewidths, isotope effects, and pressure dependence observed in Raman scattering experiments, it does not explain the structural disorder observed in the neutron diffraction experiments.

A competing model predicts that the TO(β) mode arises from the occupation of off-center [111] sites by Cu ions [4,7,13], with the cations that occupy the normal zinc blende lattice sites giving rise to the TO(γ) mode. Recent density functional (DF) calculations have shown that there are indeed secondary minima along the [111] directions in the potential felt by the Cu ions [3,15,16]. While earlier studies focused on the displacement of a single Cu ion in 8 or 16 atom supercells [3,15], Park and Chadi [16] found that extended defects involving as many as four contracted Cu atoms are energetically favorable in a 32 atom supercell. They also predicted that the concentration of these defects increases with pressure, which is inconsistent with the observed decrease in the intensity of TO(β) mode with increasing pressure [7,17,18]. In addition, while these DF calculations provide a physical justification for the static off-center model, they are not able to predict any dynamical properties.

In this paper, we present the results of *ab initio* molecular dynamics (MD) simulations of the CuCl system. The electrons are treated quantum mechanically using DF theory, while the ions move classically with forces derived from the electron-ion and ion-ion interactions. These calculations are performed at finite temperatures, so that thermal properties and the dynamics of defect formation may be studied. The use of a 64 atom supercell also permits an analysis of larger defects than density functional calculations on smaller systems [3,15,16]. At low temperatures and pressures, we find that CuCl is statically disordered with most of the Cu atoms located in off-center sites. These defects are removed with increasing temperature, making a gradual transition from static to dynamic disorder. The pressure dependence of the relative energies of the zinc blende lattice and structures containing off-center defects is also reported.

 0031-9007/99/83(3)/568(4)$15.00

The total energy and forces on the atoms were calculated within the generalized gradient [19] approximation (GGA) to density functional theory using the *ab initio* total-energy and molecular-dynamics program VASP (Vienna *ab initio* simulation program) [20]. The ions are represented by ultrasoft pseudopotentials [21]. Zero-point effects are not included in the MD simulations; however, quasiharmonic estimates of the quantum and classical free energies, using a finite difference calculation of the vibrational spectra, reveal at most a 10% zero-point correction to the differences between the free energies of the zinc blende and disordered structures at 20 K. In addition, the differences between the quantal and classical free energies are negligible above 100 K.

A kinetic energy cutoff of 234 eV was used for the plane-wave expansions. While this is lower than other DF calculations on this system, it yields energies that are accurate to within 0.1 eV per 64 atom cell. For an eight atom supercell with the zinc blende structure and a $(4 \times 4 \times 4)$ k-point sample of the Brillouin zone [22], a lattice constant of $a_0 = 5.44$ Å, a bulk modulus of 0.55 Mbar, and a cohesive energy of $E_{\text{coh}} = 6.38$ eV/CuCl pair (relative to the spin-polarized energy of isolated Cu and Cl ions) were obtained. The MD simulations were performed using a larger 64 atom supercell, a 10 fs time step, and the Γ point in the Brillouin zone; this yields a lattice constant of $a_0 = 5.42$ Å and a cohesive energy of $E_{\text{coh}} = 6.35$ eV for the zinc blende structure. The effect of using the Γ point in the Brillouin zone sample was investigated by relaxing the structures obtained from the MD simulations using the Γ point $(2 \times 2 \times 2)$ and $(4 \times 4 \times 4)$ k-point meshes. In each case, the band gap minimum was at $k = 0$ and had values ranging from 0.56 to 1.10 eV. We also repeated one of the Γ-point MD runs using a $(2 \times 2 \times 2)$ k-point mesh and found no discernible differences in the radial distribution functions (RDFs) or trajectories.

A series of simulations were performed to investigate possible low temperature structures of CuCl. A preliminary simulation was performed at 100 or 300 K to thermalize the zinc blende lattice, and the system was then cooled to 20 K with an intermediate annealing step at 100 K. Quantal effects are expected to be significant at 20 K, but the average positions at this temperature yield a structure that can be relaxed using conjugate gradient techniques. The zinc blende lattice was also used as the initial configuration in simulations at 20 and 100 K to determine the influence of the initial temperature on the resulting structure. The duration of a typical simulation was 1 ps, but the 20 K simulations were extended to 3 ps to obtain accurate equilibrium positions. Examination of the RDFs for different portions of the trajectory indicates that equilibration occurs in $\sim$0.4 ps, although this is a rough indication of structural relaxation.

The RDFs, $g(r)$, for the stepped relaxation from 300 to 20 K are shown in Fig. 1 for the Cu-Cu and Cu-Cl displacements at each temperature. Each curve was calculated by averaging over the last 0.6 ps of the trajectories. The Cu-Cl results indicate that the bond length between the Cu and Cl ions has very little temperature dependence, although a weak shoulder is evident at 300 K. The results are dramatically different for the Cu-Cu displacements. The RDF at 20 K has three distinct peaks at 2.7, 3.9, and 4.4 Å, compared to the single 3.8 Å peak expected for the zinc blende lattice. All three peaks broaden with increasing temperature, with the latter two peaks merging into a single broad feature. The intensity of the 2.7 Å peak decreases rapidly with increasing temperature, but is still evident at 300 K.

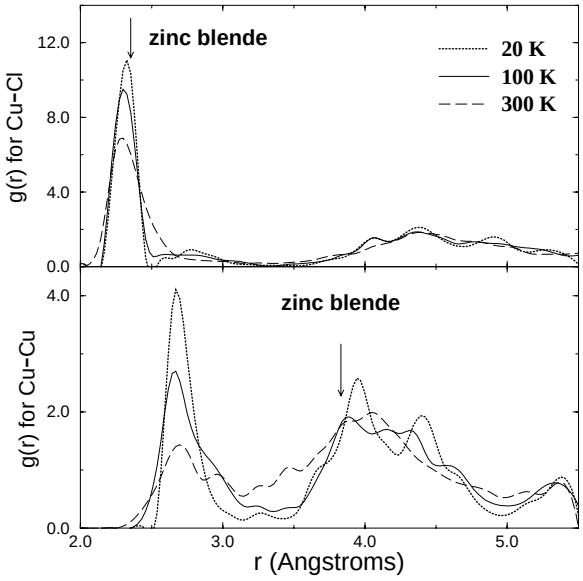

FIG. 1. Radial distribution functions, $g(r)$, for the Cu-Cu and Cu-Cl displacements at 20, 100, and 300 K. The arrows indicate the positions of the peaks expected for a zinc blende lattice.

The radial distribution functions provide information about the average environment of the Cu ions, but it is also useful to examine the individual atomic displacements to determine the origin of the peaks in $g(r)$. Using the notation introduced by Park and Chadi [16], with the number of Cu atoms in each complex represented by a subscript, the structure that yields the RDFs in Fig. 1 contains one Cu_2, one Cu_3, and three Cu_4 defects, as well as an extended Cu_7 defect that consists of two Cu_3 defects bridged by a seventh Cu atom. A cutoff of 3.3 Å, intermediate between the Cu-Cu bond lengths in CuCl and metallic Cu, was used to determine the participating Cu atoms in each defect. The mean values and distributions of the separations between the Cu and Cl ions accounts for the positions and widths of the peaks in the RDFs plotted in Fig. 1.

The displacement of the bridging atom in the Cu_7 defect is along the [100] direction, which is equivalent to a superposition of displacements along two of the [111] directions. This defect is shown in Fig. 2, with the Cu atoms represented by small shaded circles and

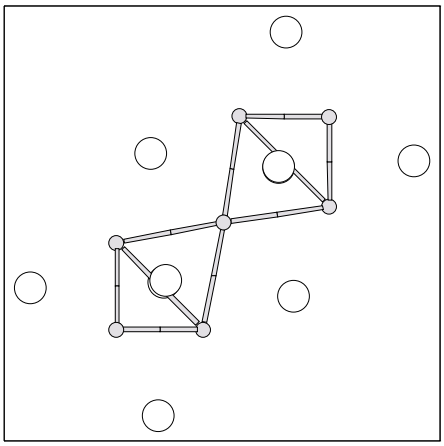

FIG. 2. Structure of the Cu_7 complex. The Cu atoms are represented by the small shaded circles, while the large open circles are the nearest neighbor Cl atoms.

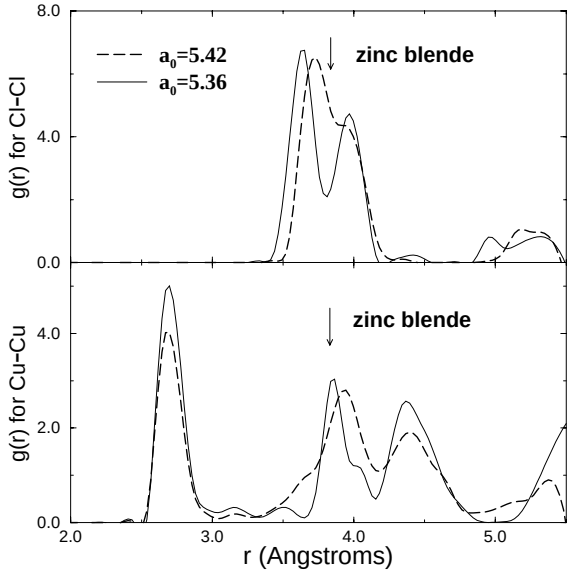

FIG. 3. Radial distribution functions, $g(r)$, for the Cu-Cu and Cl-Cl displacements at 20 K with different lattice constants. The arrows indicate the position of the peak expected for a zinc blende lattice with the larger lattice constant.

their nearest-neighbor Cl atoms by the larger open circles. The Cu atom in the center of Fig. 2 is displaced by 0.9 Å relative to the zinc blende lattice, while the average displacement of the other Cu atoms is 0.7 Å. The average separation of the Cu atoms linked by the shaded "bonds" is 2.72 Å, while the average Cu-Cl bond length is 2.31 Å, nearly equal to the 2.35 Å separation in the zinc blende lattice. The coordination number of the bridging Cu atom has decreased from 4 to 2 compared to the zinc blende lattice, while the other Cu atoms in the defect now have three nearest Cl neighbors.

At high pressures, it has been observed that the Raman intensity of the TO(β) mode decreases with respect to that of the TO(γ) mode [4,17,18]. This pressure dependence has been reproduced with the Fermi resonance model, but DF calculations have predicted that the concentration of off-center defects increases with increasing pressure [16]. This finding is inconsistent with experiment if it is assumed that these defects are responsible for the anomalous TO(β) mode. The simulations that produced the RDFs plotted in Fig. 1 were performed with a lattice constant of 5.42 Å, which resulted in an average external pressure of $+0.3$ GPa relative to the zinc blende lattice. Reducing the lattice constant to 5.36 Å yielded a relative pressure of $+1.0$ GPa, and the RDFs for the resulting structure are compared to those for $a_0 = 5.42$ Å in Fig. 3. The Cu-Cu displacements again result in three peaks near 2.7, 3.85, and 4.4 Å, but the latter two are significantly sharper with the smaller lattice constant. This effect is even more pronounced for the Cl-Cl displacements, with the broad 3.85 Å peak split into two distinct peaks at 3.65 and 3.95 Å when the lattice constant decreases. This behavior indicates that an increase in the external pressure significantly reduces the disorder, but the strong Cu-Cu peak near 2.7 Å indicates that most of the Cu atoms remain at off-center sites. The differences between the RDFs plotted in Fig. 3 can be traced to correlations in the Cu displacements. The structure with the smaller lattice constant consists of four Cu_7 (see Fig. 2 complexes symmetrically arranged in the 64 atom supercell, with the remaining four Cu atoms located at zinc blende sites.

The 300 K temperature used in the initial simulations enables the Cu atoms to dynamically explore all of the [111] off-center sites. We expect this motion to be restricted at lower temperatures, so we performed a final series of simulations with initial temperatures of 20 and 100 K. At 20 K, there is no deviation from the zinc blende structure during a 3 ps simulation, which indicates that this is also a possible metastable configuration. However, when the zinc blende lattice was annealed at 100 K, the system evolved into a random distribution of six Cu_4 defects. The RDFs for the Cu-Cu displacements in this configuration are very similar to those plotted for the 5.42 Å lattice constant in Fig. 2.

We next employed a conjugate gradient method to relax the four structures described in this work: zinc blende, disordered (correlated defects of different sizes that generated the RDFs in Fig. 1), $4 \times Cu_7$ (an ordered array of four Cu_7 defects) and $6 \times Cu_4$ (a random distribution of six Cu_4 defects). These structures represent just four possible arrangements of Cu atoms situated at zinc blende and off-center sites. These configurations were relaxed using a $(4 \times 4 \times 4)$ k-point mesh and a kinetic energy cutoff of 234 eV. At zero pressure, the disordered structure has a total energy of -1.3 eV compared to the zinc blende lattice, but this increases to -1.0 and -0.6 eV as the pressure increases to 0.9 and 2.9 GPa, respectively. The lowest total energy relative to the zinc blende lattice was obtained with the $6 \times Cu_4$ structure, and this increased from -1.7 eV at zero pressure to -0.9 eV at 2.9 GPa. The energy of the $4 \times Cu_7$ structure is 0.1 eV

higher than the $6 \times Cu_4$ structure at each pressure. Although the structures containing off-center defects are energetically favored over the zinc blende lattice, the energy differences decrease by a factor of 2 as the pressure increases from 0 to 2.9 GPa. This indicates that pressure may reduce the number of off-center defects, in qualitative agreement with experiment. In addition, at zero pressure, the lattice constants of the $6 \times Cu_4$ and zinc blende structures are 5.41 and 5.395 Å, respectively. The relative sizes indicate that CuCl will contract as the off-center defects are removed with increasing temperature. This effect would partially compensate the thermal expansion at low temperatures and is consistent with a negative thermal expansion in this regime [2].

Examination of the MD trajectories is useful for determining the driving mechanism behind the formation of these defects. At 300 K, the Cu ions are very mobile and are found in any of the off-center sites with equal probability. As the temperature decreases, some of these atoms become trapped in these off-center sites, which decreases their Cu-Cl coordination numbers from 4 to 3. These off-center defects then lower the barrier for the trapping of their nearest Cu neighbors in correlated off-center sites. This process continues until the majority of the Cu ions have formed Cu_4 or Cu_7 complexes. This is consistent with an explanation [16] for the driving mechanism of Cu_4 defect formation where the breaking of bonds between Cu and Cl atoms results in a strong hybridization of the Cu d states that favors an increase in the overlap between the wave functions of neighboring Cu atoms. Projections of the valence bands onto s, p, and d orbitals confirms this analysis and also indicates that many of the electronic states are localized on the Cu defects. The vibrational frequencies of CuCl were not addressed in this work, but the off-center displacements are expected to produce Raman active modes [4,7] that would be dynamically coupled to the TO(γ) mode as the Cu atoms move between off- and on-center sites. Because of the strong interactions between Cu atoms in the off-center defects, the modes involving these atoms would be strongly localized with frequencies that depend on the isotopic masses, in agreement with recent Raman experiments [23].

To summarize, *ab initio* MD simulations have resolved several questions about the structure of CuCl. At low temperatures and pressures, the lattice contains disorder as well as correlation between the off-center Cu atom displacements. This finding is consistent with the prediction that correlated off-center displacements are needed to reproduce the diffuse background in neutron diffraction experiments [10]. Moderate external pressures tend to reduce the disorder and decrease the energy differences between the zinc blende lattice and lattices containing off-center defects. Although the large vibrational amplitudes of the Cu atoms indicate that anharmonicity is important, the disorder and temperature dependence of the off-center displacements are sufficient to account for the dynamical properties without introducing a Fermi resonance. We also note that while most of the Cu ions are displaced in off-center sites at low temperatures, the net dc dipole moment vanishes due to symmetry. The dc dielectric constant would therefore not exhibit the Curie-Weiss behavior observed in ferroelectric crystals near a displacive phase transition.

This work was performed under the auspices of the Department of Energy at the Theoretical Division of the Los Alamos National Laboratory.

[1] J. C. Phillips, *Bonds and Bands in Semiconductors* (Academic Press, New York, 1973).
[2] J. N. Plendl and L. C. Mansur, Appl. Opt. **11**, 1194 (1972); J. N. Plendl, A. Hadni, J. Claudel, Y. Henninger, G. Morlot, P. Strimer, and L. C. Mansur, Appl. Opt. **5**, 397 (1966).
[3] S.-H. Wei, S. B. Zhang, and A. Zunger, Phys. Rev. Lett. **70**, 1639 (1993).
[4] Z. Vardeny and O. Brafman, Phys. Rev. B **19**, 3276 (1979).
[5] I. P. Kaminow and E. H. Turner, Phys. Rev. B **5**, 1564 (1972); E. H. Turner, I. P. Kaminow, and C. Schwab, Phys. Rev. B **9**, 2524 (1974).
[6] J. E. Potts, R. C. Hansen, C. T. Walker, and C. Schwab, Phys. Rev. B **9**, 2711 (1974); B. Prevot, B. Hennion, and B. Dorner, J. Phys. C **10**, 3999 (1977).
[7] G. Livescu and O. Brafman, Phys. Rev. B **34**, 4225 (1986).
[8] G. Kanellis, W. Kress, and H. Bilz, Phys. Rev. B **33**, 8724 (1986); **33**, 8733 (1986).
[9] M. Sakata, S. Hoshino, and J. Harada, Acta Crystallogr. Sect. A **30**, 655 (1974).
[10] J. Schreurs, M. H. Mueller, and L. H. Schwartz, Acta Crystallogr. Sect. A **32**, 618 (1976).
[11] S. Hull and D. A. Keen, J. Phys. Condens. Matter **8**, 6191 (1996).
[12] J. B. Boyce, T. M. Hayes, and J. C. Mikkelson, Jr., Phys. Rev. B **23**, 2876 (1981).
[13] S. Miyake, S. Hoshino, and T. Takenaka, J. Phys. Soc. Jpn. **7**, 19 (1952).
[14] M. Krauzman, R. M. Pick, H. Poulet, G. Hamel, and B. Prevot, Phys. Rev. Lett. **33**, 528 (1974).
[15] C.-Z. Wang, R. Yu, and H. Krakauer, Phys. Rev. Lett. **72**, 368 (1994).
[16] C. H. Park and D. J. Chadi, Phys. Rev. Lett. **76**, 2314 (1996).
[17] H. D. Hochheimer, M. L. Shand, J. E. Potts, R. C. Hanson, and C. T. Walker, Phys. Rev. B **14**, 4630 (1976).
[18] C. Ulrich, A. Göbel, K. Syassen, and M. Cardona, Phys. Rev. Lett. **82**, 351 (1999).
[19] J. P. Perdew, K. Bukre, and M. Ernzhof, Phys. Rev. Lett. **77**, 3865 (1996).
[20] G. Kresse and J. Hafner, Phys. Rev. B **47**, 558 (1993); **49**, 14 251 (1994); G. Kresse and J. Furthmüller, Phys. Rev. B **54**, 11169 (1996).
[21] D. Vanderbilt, Phys. Rev. B **41**, 7892 (1990); G. Kresse and J. Hafner, J. Phys. Condens. Matter **6**, 8245 (1994).
[22] H. J. Monkhorst and J. D. Pack, Phys. Rev. B **13**, 5188 (1976).
[23] A. Göbel, T. Ruf, C.-T. Lin, M. Cardona, J.-C. Merle, and M. Joucia, Phys. Rev. B **56**, 210 (1997).